Tissue Characterization in Ultrasound

Dr. Debdoot Sheet
Assistant Professor, Department of Electrical Engineering
Principal Investigator, Kharagpur Learning, Imaging and Visualization Group
Indian Institute of Technology Kharagpur

www.facweb.iitkgp.ernet.in/~debdoot/

Contents

Introduction

- Human body consists of organs and systems made up of different tissues.
- Pathological conditions and abnormalities affect their normal functioning.
- Critical soft tissue abnormalities include
  - Plaque formation in the blood vascular system.
  - Lesions in the breast.
  - Degeneration of the retina.
  - Wounds in the skin.
- Traditional practice of Histopathological diagnosis requires invasive Biopsy / Excision for tissue collection
  - Not possible in vessels in living Humans
  - Improper sampling from Breast lesion affects diagnostic outcome
  - Not possible in retina in living Humans
  - Not possible in healing wounds.

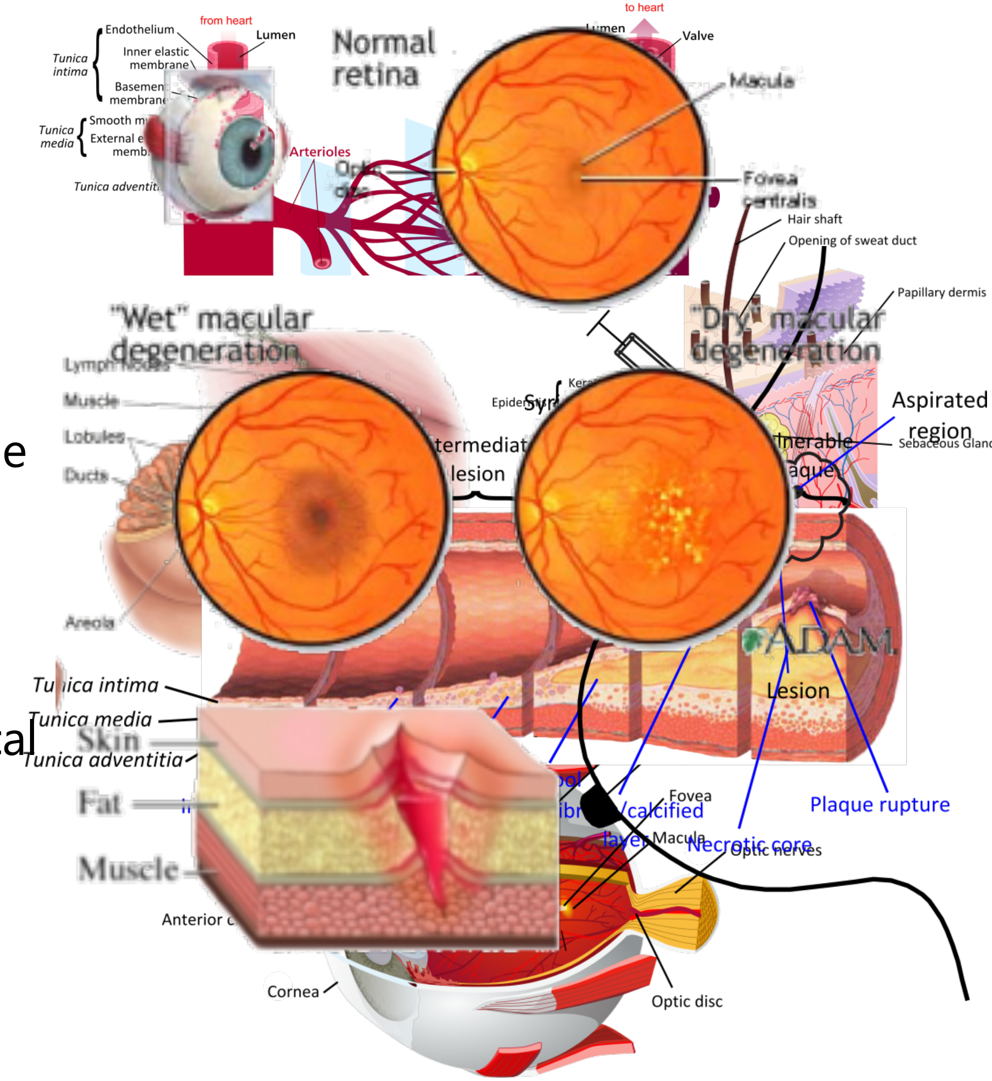

Blood Vascular System

- Atherosclerosis
  - Plaque builds up in arteries
  - Forms anywhere in the vascular system
- Cardiovascular diseases (CVD)
- *In vivo* Imaging of Plaques
  - CT Angiography (CTA)
  - MR Angiography (MRA)
  - **Intravascular Ultrasound (IVUS)**
  - Intravascular OCT (IV-OCT)
  - Intravascular Near-Infrared Spectroscopy (NIR)
- Plaque Vulnerability Assessment
  - Calcification, fibrosis identification
  - Lipid pool and Necrosis burden estimation

- Spectral analysis of received ultrasonic echo signal
  - Lizzi et al., 1983
  - Nair et al., 2001
  - Kawasaki et al., 2002
  - Virtual Histology (Volcano Corp.)
  - iMap (BostonScientific)
- Texture analysis of B-mode image/signal
  - Katouzian et al., 2008, 2010, 2012 (Prog. Hist. / PH)
  - Esclara et al., 2009
  - Seabra et al., 2011
- Limitations
  - Unable to identify heterogeneous tissue composition
  - Cannot discriminate between dense fibrous tissue and calcification
  - Fails to discriminate true necrosis from shadows

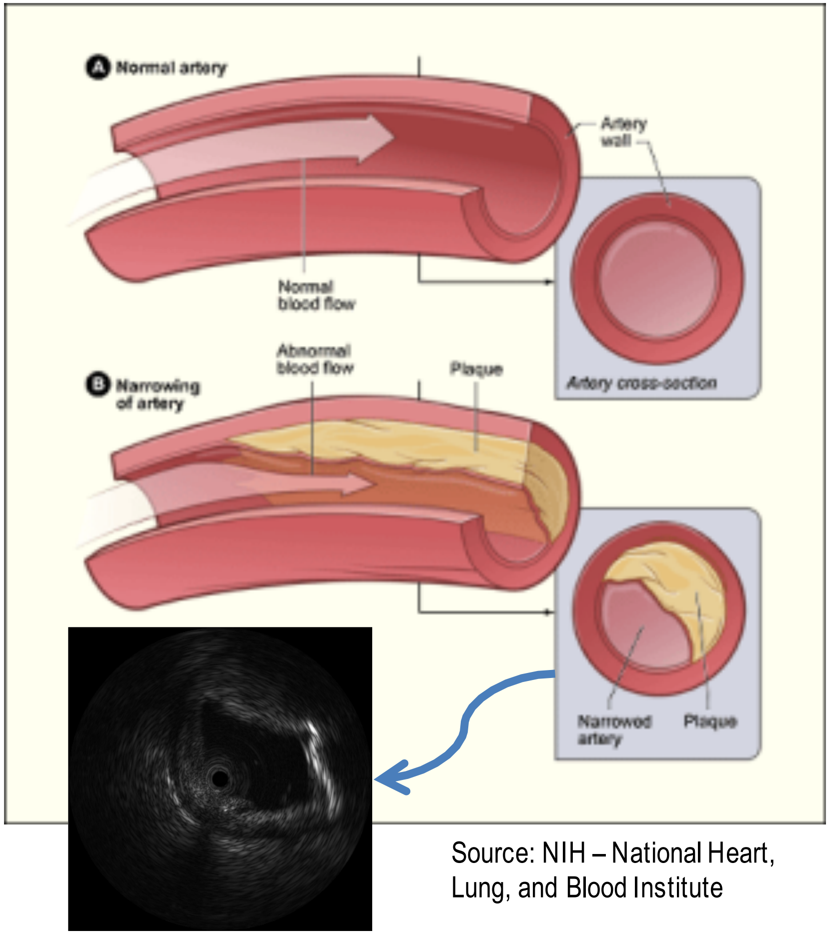

Source: NIH – National Heart, Lung, and Blood Institute

Backdrop

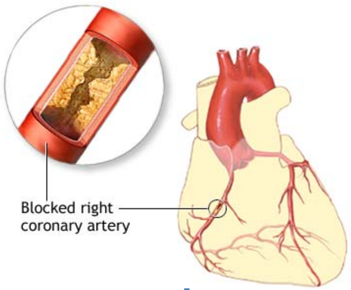

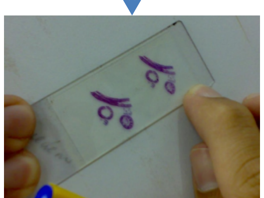

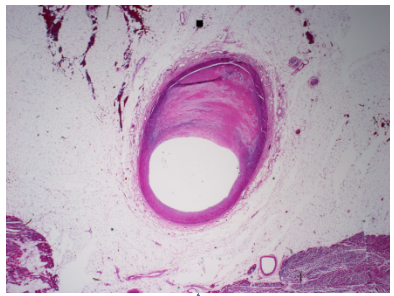

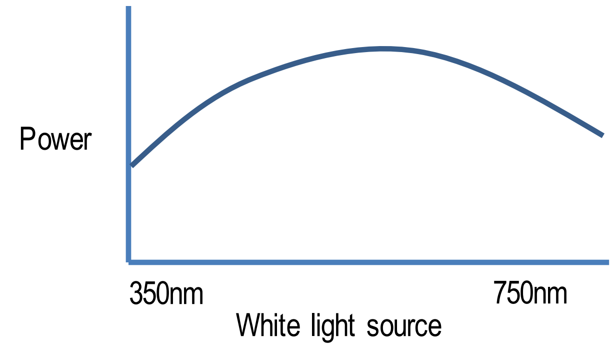

Stained tissue section

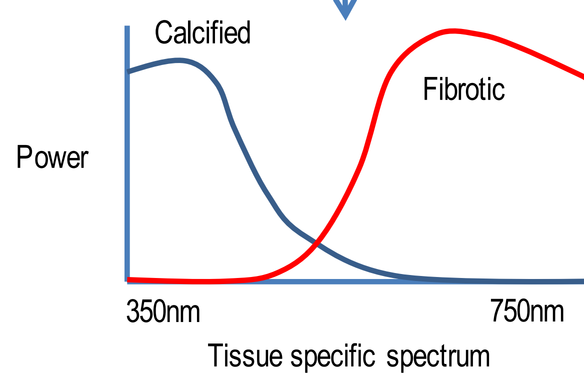

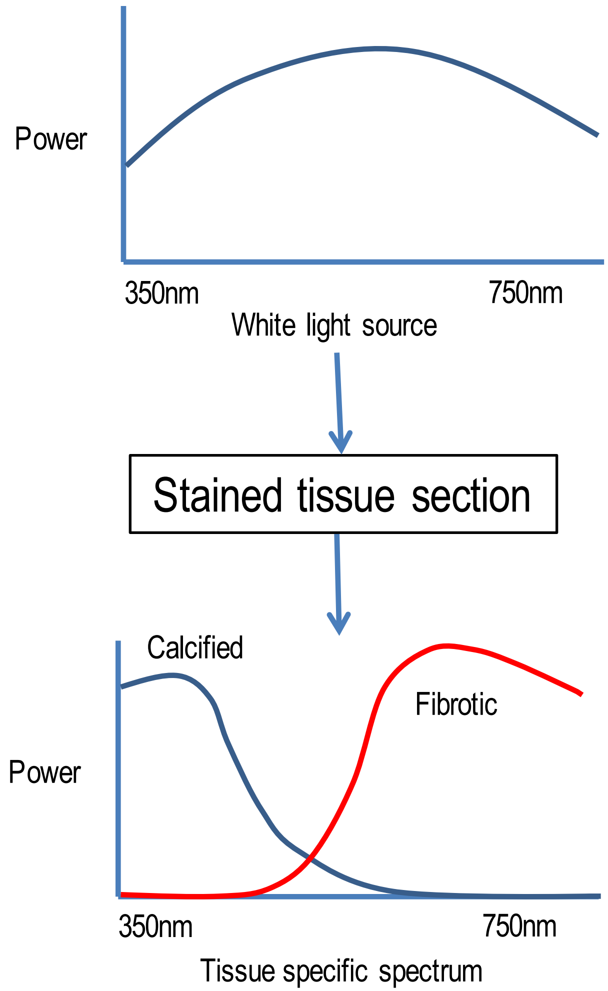

: Probing energy (Light)

: Physiological property (Tissue type)

$$= f(\quad)$$

$$= f^{\ 1}(\quad)$$

Inferring tissue type based on color

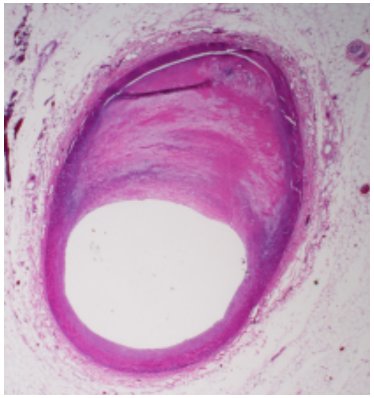

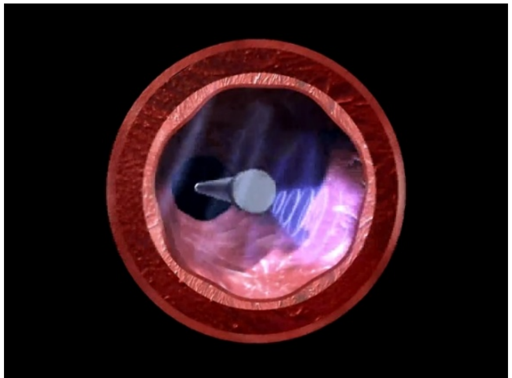

: Probing energy (Acoustic)

: Tissue type (Backscatterer density)

$$= f(\quad)$$

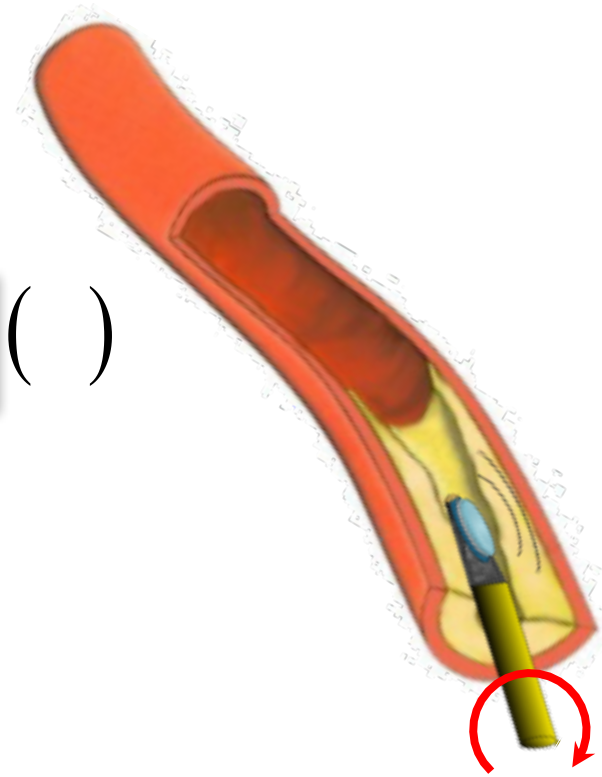

Computation Modelling of Tissue Energy Interaction for *In situ* Histopathology

$$= \boxed{f}^{\,1}(\quad)$$

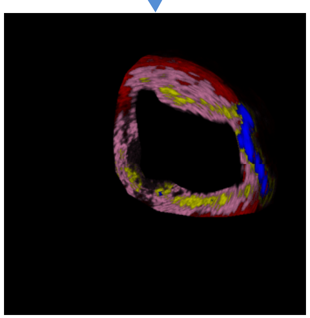

Computed histology

Inferring tissue type based on backscattering response

Limited Resolution Challenge

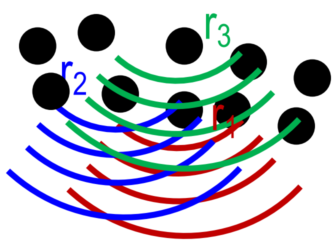

$$\ _{r_1} = f\left(\ _{r_1} \right)$$
$$\ _{r_2} = f\left(\ _{r_2} \right)$$
$$\ _{r_3} = f\left(\ _{r_3} \right)$$

Ultrasound signal backscattered within a resolution cell

$$= E\left(\ _{r_i} \right)$$
$$= E\left(f\left(\ _{r_i} \right)\right)$$

Signal sensed by the transducer

$$\hat{\ } = f^{\ 1}\left(E\left(f\left(\ _{r_i} \right)\right)\right)$$

Estimated functional ensemble of backscatterer density

$$\hat{\ }$$

Improper estimation of tissue type in inhomogeneous media

P. M. Shankar, “A general statistical model for ultrasonic backscattering from tissues”, *IEEE Trans. Ultrasonics, Ferroelectrics, Freq. Control.*, vol. 47, no. 3, pp. 727-736, May 2000.

Statistical Physics in Acoustic Imaging

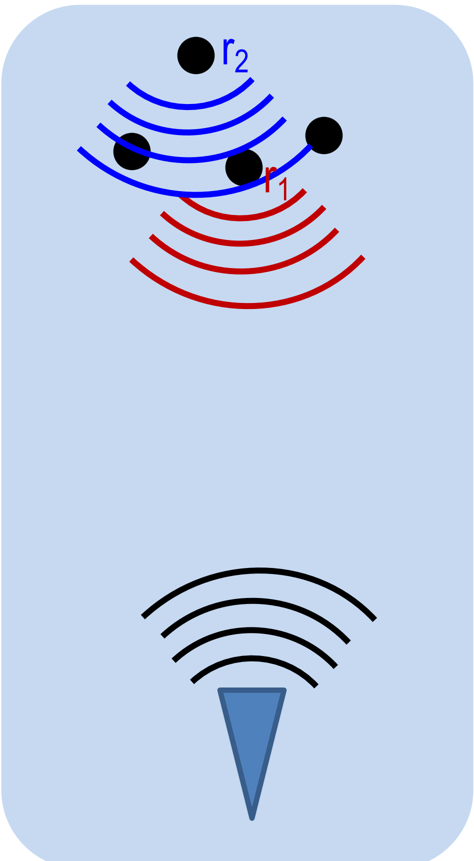

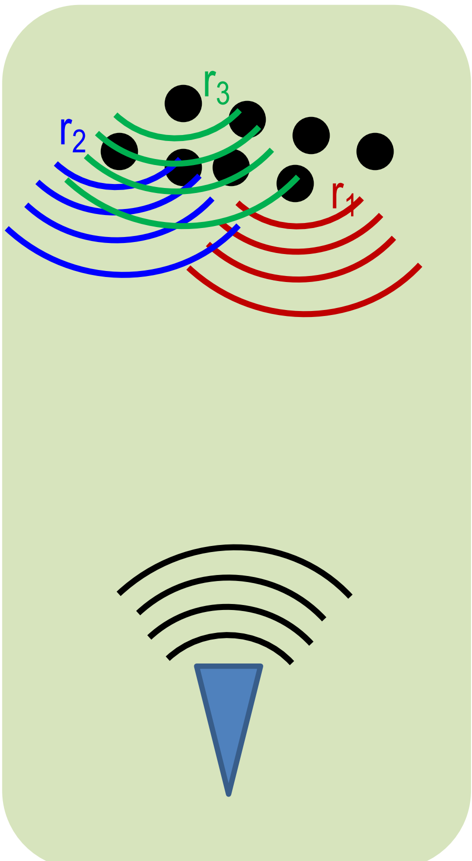

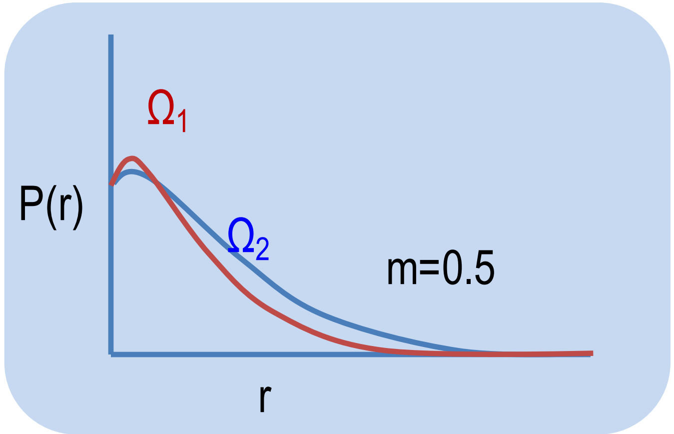

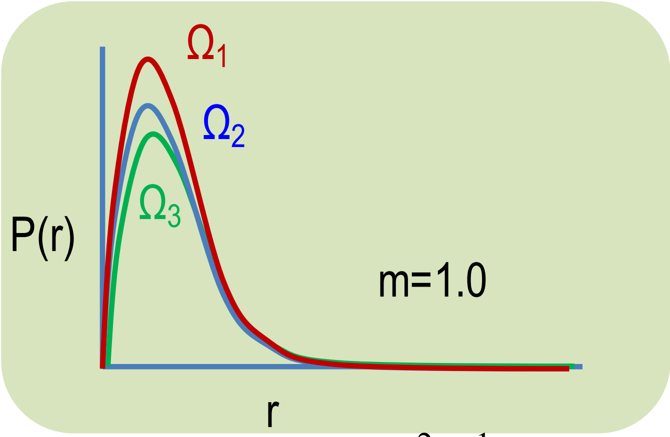

P. M. Shankar, "A general statistical model for ultrasonic backscattering from tissues", *IEEE Trans. Ultrasonics, Ferroelectrics, Freq. Control.*, vol. 47, no. 3, pp. 727-736, May 2000.

$$\mathcal{N}(r\mid m,\quad)=\frac{2m^{m}r^{2m\quad 1}}{(m)\quad^{m}}\exp\quad\frac{m}{\quad}r^{2}$$

Statistical physics of ultrasonic backscattering

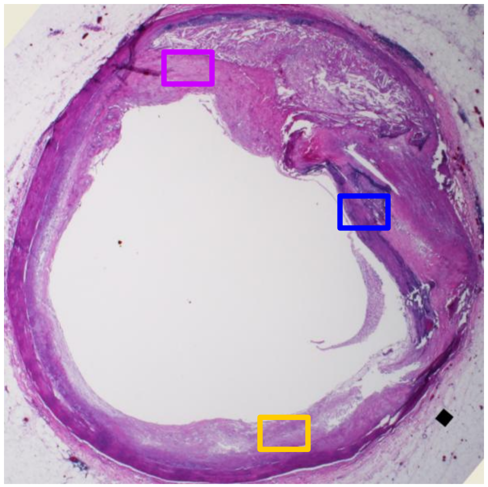

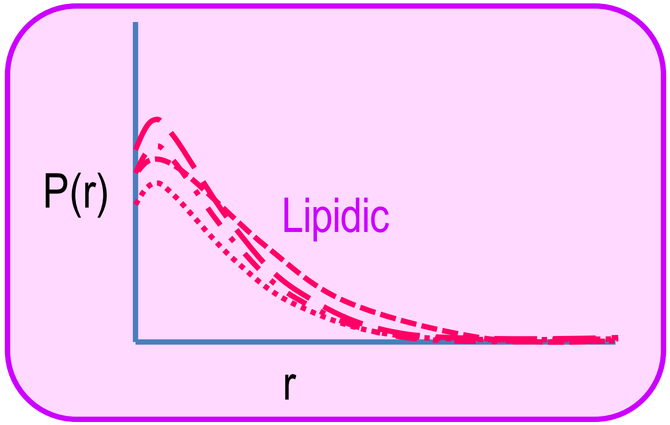

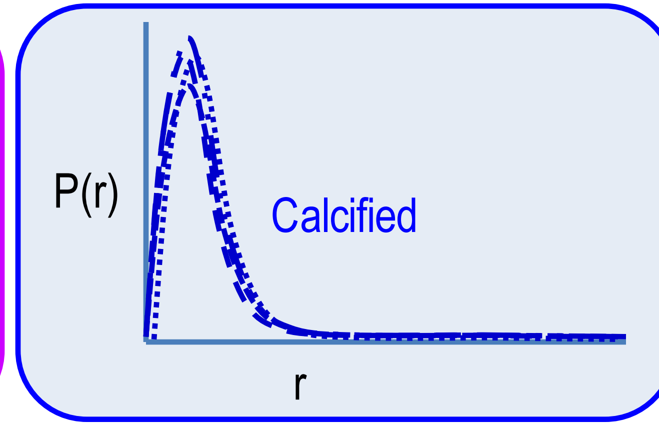

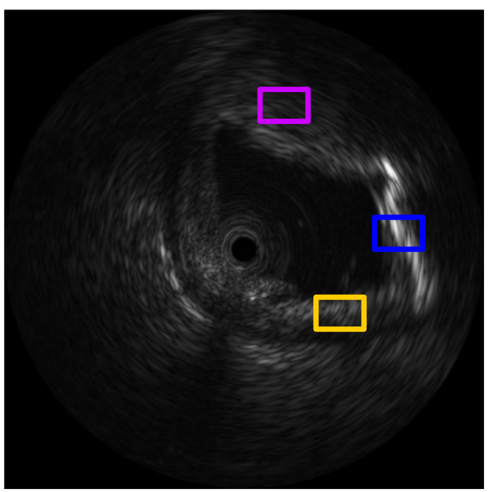

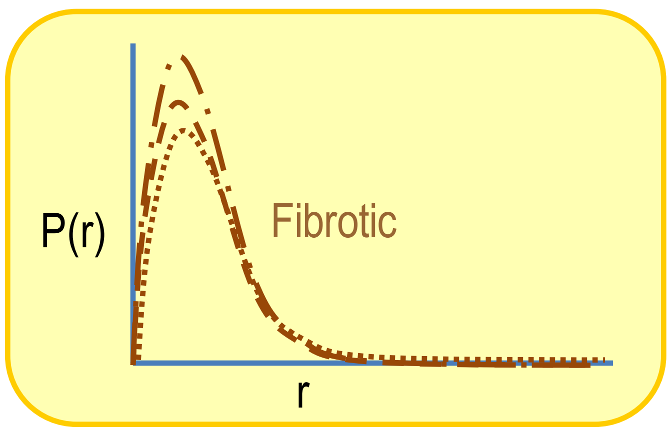

V. Dumane and P. M. Shankar, "Use of frequency diversity and Nakagami statistics in ultrasonic tissue characterization", *IEEE Trans. Ultrasonics, Ferroelectrics, Freq. Control*, vol. 48, no. 4, pp. 1139-1146, Jul. 2001

F. Destrempes, J. Meunier, M. . F. Giroux, G. Soulez, G. Cloutier, "Segmentation in ultrasonic b-mode images of healthy carotid arteries using mixture of Nakagami distributions and stochastic optimization", *IEEE Trans. Med. Imaging*, vol. 28, no. 2, pp. 215-229, Feb. 2009.

Mathematical intractability, *the problem*

$$p(y\,|\,r) = \frac{p(r\,|\,y)}{p(r)} P(y)$$ Th decision making framework

$$p(r\,|\,y) = f(r\,|\,(p_1,\ldots,m_1,\ldots,\;{}_1,\ldots)\;\ldots),\ldots;y)$$

$$= {}_{l=1}^{\boxed{L}}\ \boxed{p_{l,}}\,\mathcal{N}(r\,|\;{}_l, m_l)$$

Scales unknown

Correlation among scales unknown

No. components unknown

Prior probab. of each comp. unknown

Proposed Solution

$$p(y \mid \boxed{}, r) = \frac{p(\boxed{}, r \mid y)}{p(\boxed{}, r)} P(y) = \boxed{H}(y \mid \boxed{}, \boxed{\mathcal{R}}; \boxed{\{\mathcal{R}\}_{\text{train}}})$$

Statistical physics model of ultrasonic backscattering

Set of signal received by the transducer

Training set of annotated examples to be used for supervised learning

Supervised learner for learning tissue specific statistical physics model

Solution through Transfer Learning Framework

IVUS Tissue Characterization

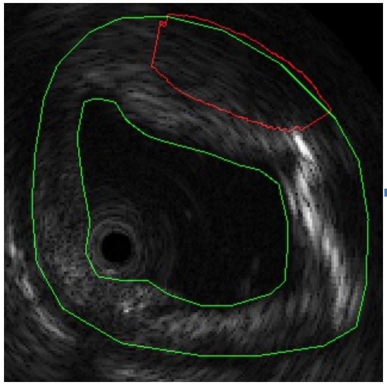

Nakagami parameter and signal confidence estimate

Random forest learning

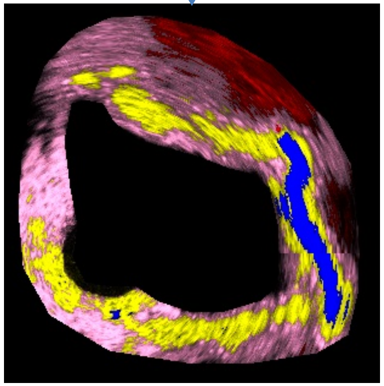

Background
Lipidic
Fibrotic
Calcified
Necrosis

Joint learning of ultrasonic backscattering statistical physics and signal confidence primal for characterizing atherosclerotic plaques using intravascular ultrasound, *Med. Image Anal*,18(1), 2014

Hunting for necrosis in the shadows of intravascular ultrasound, *CMIG*, 38(2), 2014

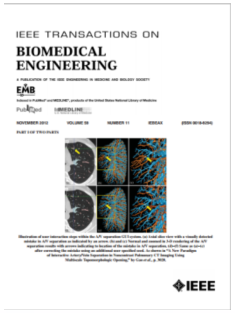

Iterative self-organizing atherosclerotic tissue labeling in intravascular ultrasound images and comparison with virtual histology, *IEEE TBME*, 59(11), 2012

Ultrasound Signal Confidence

- An ultrasonic pulse as well as backscattered echo travel along the same path through a heterogeneous media.
- They are subjected to the same attenuation.
- Confidence of the received signal is a reflection of fidelity of samples received by the transducer.
- It can be estimated by treating its propagation as a random walk along an ultrasonic scan-line.
- A random walker starting at a point on the scan-line reaches the virtual transducer element placed at the origin of each scan-line.
- This random walk is solved using the electric network equivalent and solving it in the paradigm of graph theory.

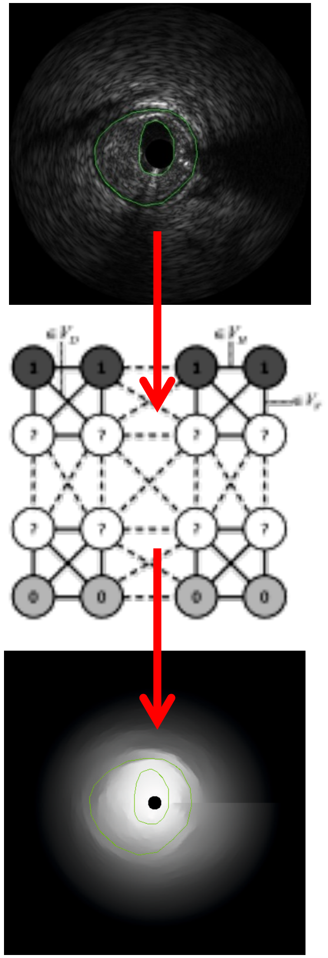

A. Karamalis, W. Wein, T. Klein, N. Navab (2012) Ultrasound confidence maps using random walks, Medical Image Analysis, **16:**1101–1112.

Transfer Learning Framework

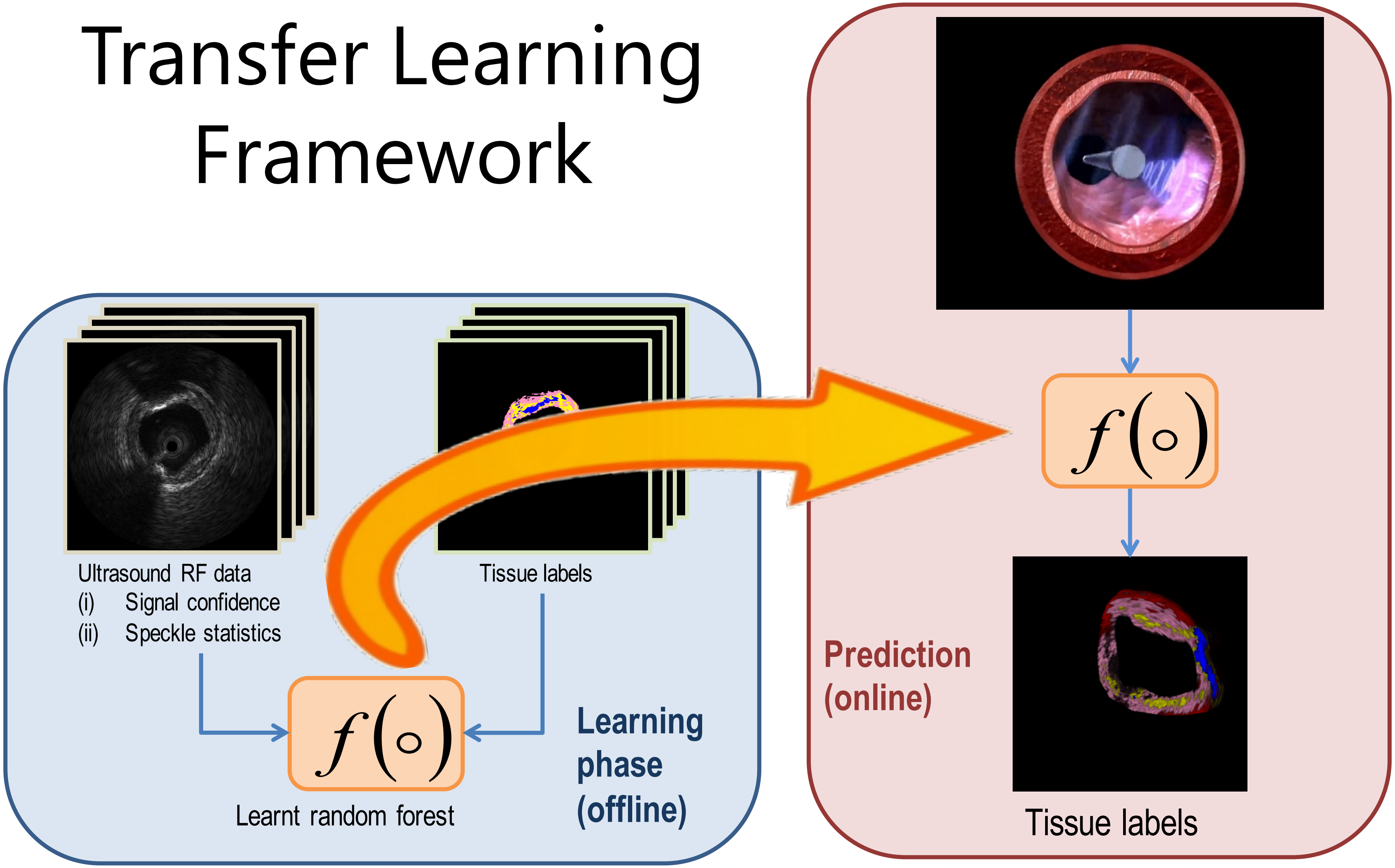

Random Forests for Learning

Training set

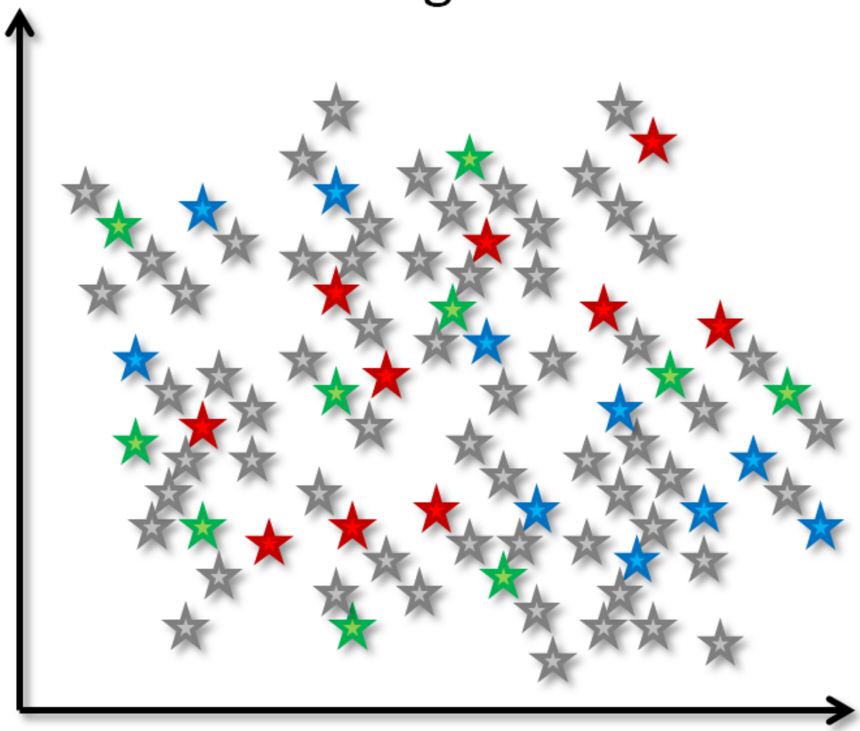

Decorrelated trees

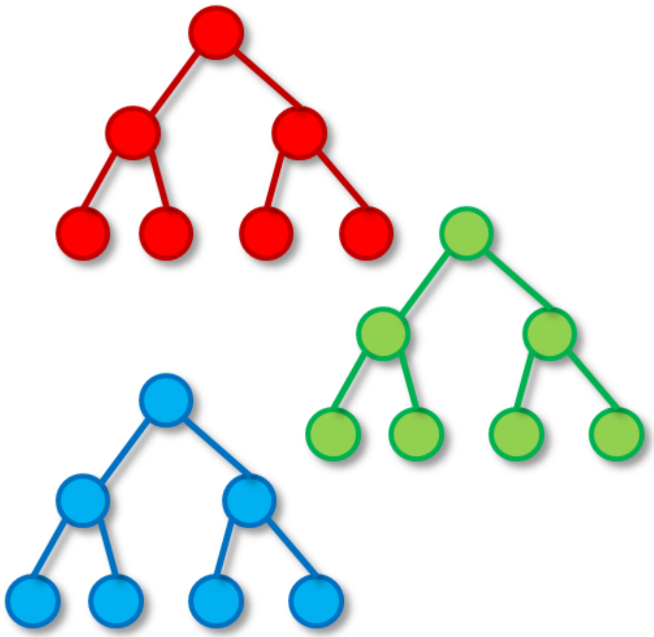

$$p(c|\mathbf{v}) = \frac{1}{T}\sum_{t}^{T} p_t(c|\mathbf{v})$$

A. Criminisi and J. Shotton, *Decision Forests for Computer Vision and Medical Image Analysis*, Springer, 2013.

Experiment Design

- Data Collection:
  - Columbia University, New York City, NY, USA
  - Interventional Cardiologist: Dr. Stephane G. Carlier
  - Cardiovascular Histopathologist: Dr. Renu Virmani, CV Path Institute, Gaithersburg, USA
  - Cases # 13
  - Tissue Sections # 53
  - Atlantis, 40 MHz IVUS, Boston Scientific,CA, USA
  - Sampling freq: 400 MHz
  - Sampling geometry: 256 scan lines per rotation, 2048 samples per scan line
- Learning
  - Source task: {Ω,m} estimated at 28 scales + Ultrasonic Confidence (A. Karamalis, et al. (2012))
  - Target task: Random forest 50 decision trees
- Cross validation
  - 53 fold cross validation
  - Learn with 52, test on the remaining

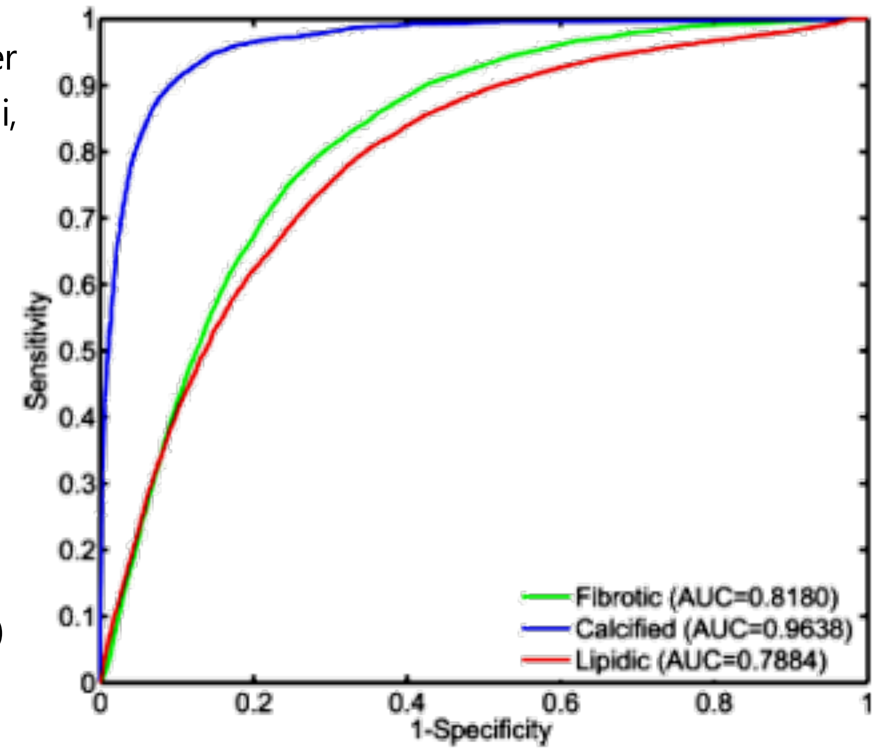

Ultrasonic Histology of Atherosclerotic Plaques

- Characterization based on ultrasonic statistical physics.
- Superior machine learning algorithm.
- Reliability measure for estimation of tissues.

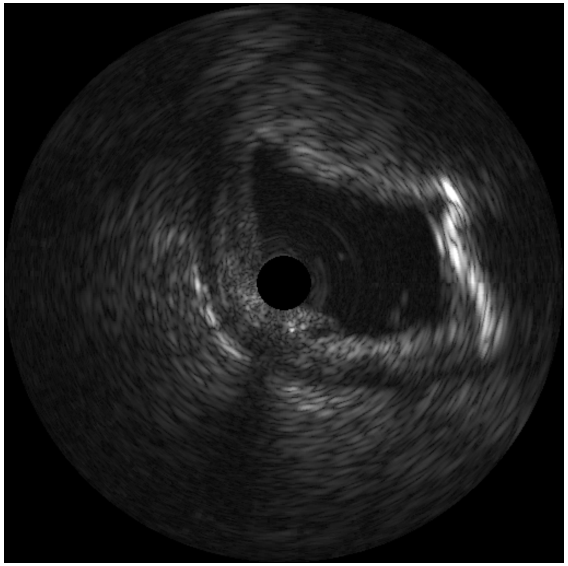

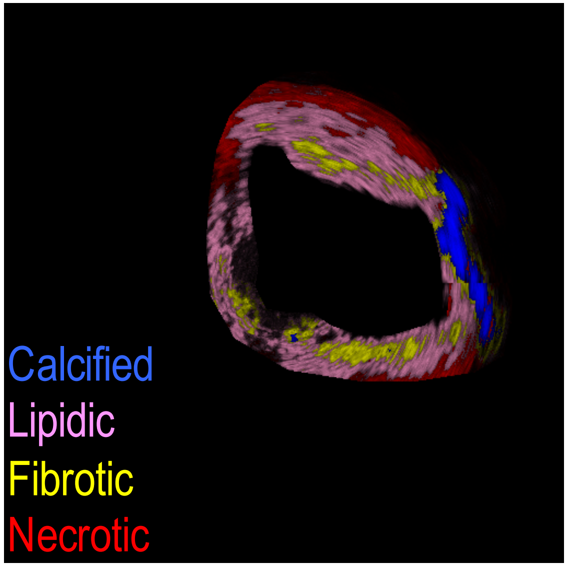

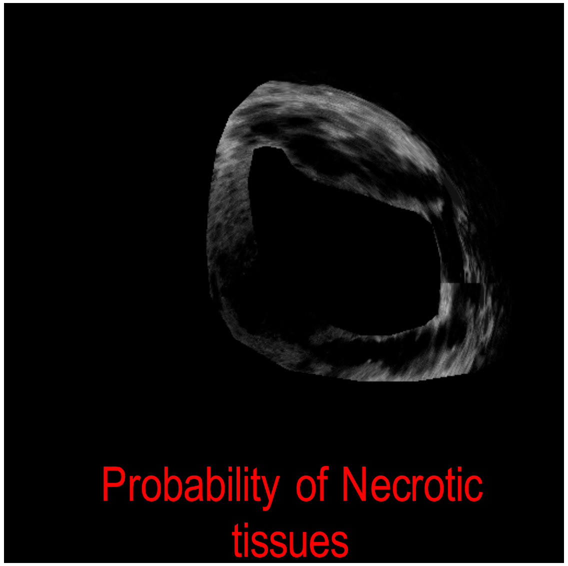

Coronary Plaque Characterization and Staging

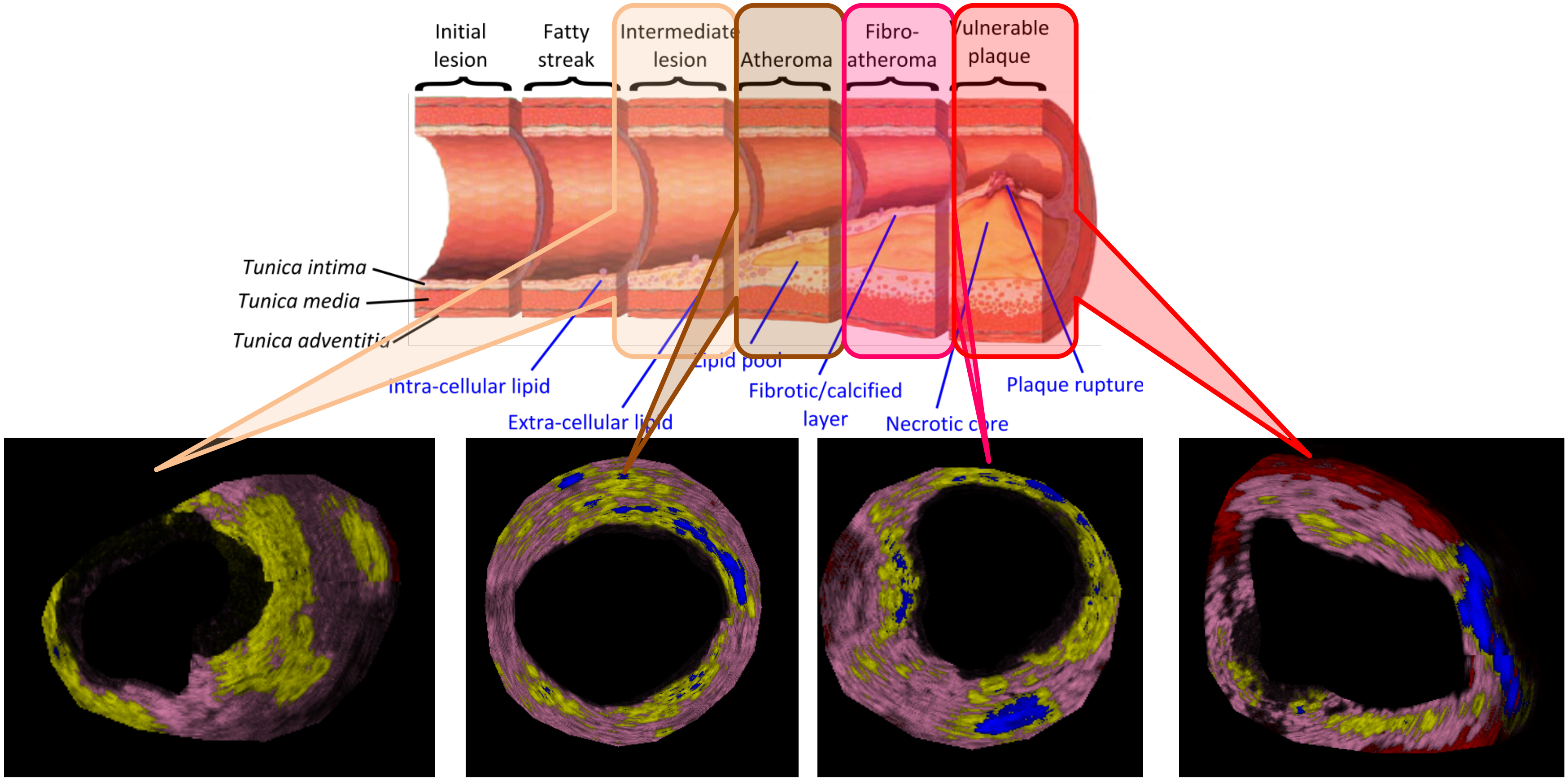

Performance Evaluation

Inter-observer variability

	Calcified		Fibrotic		Lipid	
	Obs 1	Obs 2	Obs 1	Obs 2	Obs 1	Obs 2
Calcified	**98.65 ± 1.79**	**98.48 ± 2.13**	1.17 ± 1.52	1.25 ± 1.72	0.17 ± 0.33	0.27 ± 0.51
max	100	100	15	15	6	6
min	85	80	0	0	0	0
Fibrotic	0.71 ± 0.90	0.88 ± 1.09	**96.92 ± 2.87**	**96.73 ± 2.99**	2.36 ± 2.73	2.38 ± 2.68
max	5	5	100	100	15	10
min	0	0	85	85	0	0
Lipid	0 ± 0	0 ± 0	0.71 ± 1.25	0.69 ± 1.22	**99.28 ± 1.25**	**99.30 ± 1.22**
max	0	0	10	10	100	100
min	0	0	0	0	90	90

Intra-observer variability

	Calcified		Fibrotic		Lipid	
	Day 1	Day 2	Day 1	Day 2	Day 1	Day 2
Calcified	**98.65 ± 1.79**	**99.00 ± 1.11**	1.17 ± 1.52	1.00 ± 1.53	0.17 ± 0.33	0 ± 0
max	100	100	15	10	6	0
min	85	90	0	0	0	0
Fibrotic	0.71 ± 0.90	0.91 ± 1.15	**96.92 ± 2.87**	**97.12 ± 2.45**	2.36 ± 2.73	1.98 ± 2.36
max	5	8	100	100	15	15
min	0	0	85	85	0	0
Lipid	0 ± 0	0 ± 0	0.71 ± 1.25	1.31 ± 2.01	**99.28 ± 1.25**	**98.69 ± 2.01**
max	0	0	10	10	100	100
min	0	0	0	0	90	90

S. Conjeti, A. Katouzian, A. Guha Roy, L. Peter, D. Sheet, S. Carlier, A. Laine and N. Navab, "Supervised Domain Adaptation of Random Forests: Transfer of models trained in vitro for in vivo intravascular ultrasound tissue characterization", *Medical Image Analysis*, vol. 32, no. 1, pp. 1-17, June 2016.

DOMAIN ADAPTATION

In vivo Ultrasonic Histology

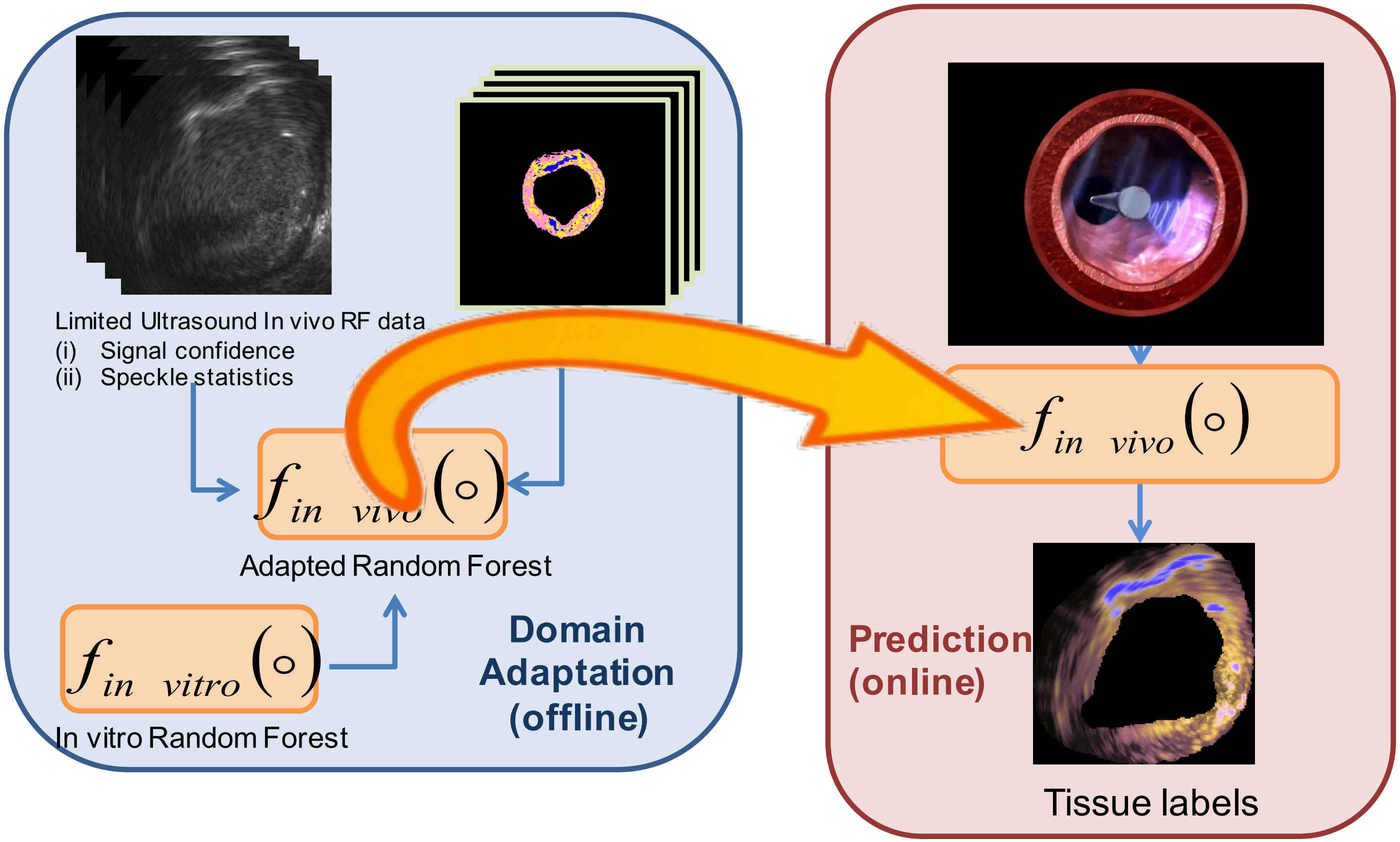

Conjeti, S., Katouzian, A., Roy, A.G., Peter, L., Sheet, D., Carlier, S., Laine, A. and Navab, N., 2016. Supervised domain adaptation of decision forests: Transfer of models trained in vitro for in vivo intravascular ultrasound tissue characterization. *Medical image analysis*, *32*, pp.1-17.

In vivo Validation – Visual Evaluation

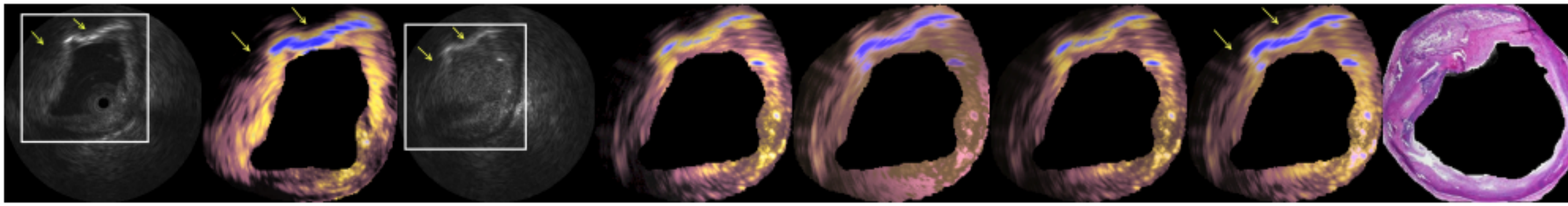

(a) *In vitro* (b) *In vitro* TC (c) *In vivo* (d) BL1 (e) BL2 (f) BL3 (g) Proposed (h) Histology

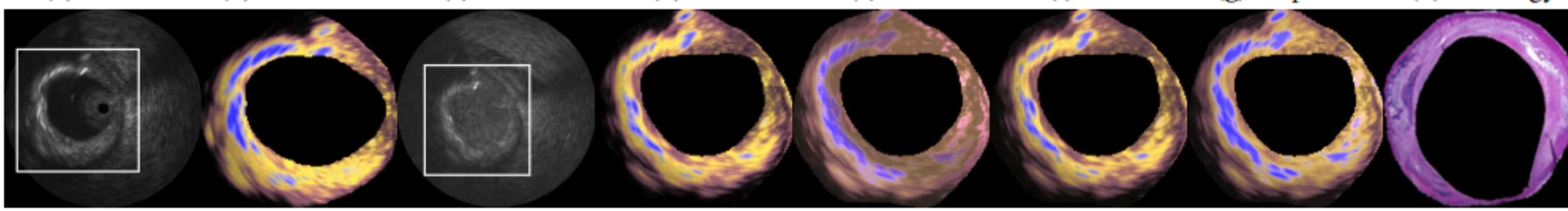

(i) *In vitro* (j) *In vitro TC* (k) *In vivo* (l) BL1 (m) BL2 (n) BL3 (o) Proposed (p) Histology

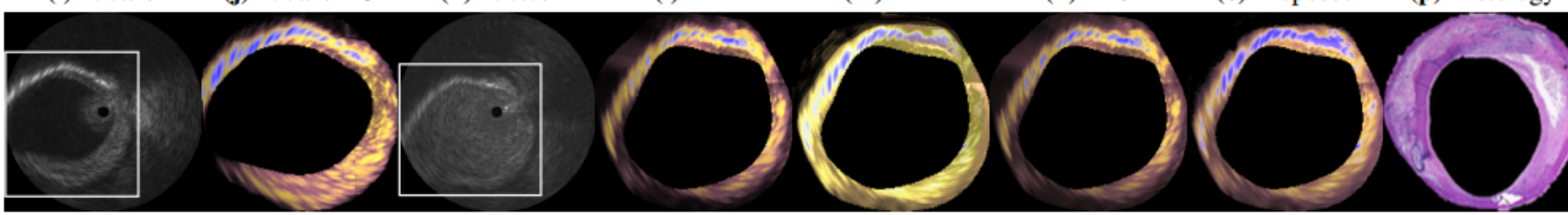

(q) *In vitro* (r) *In vitro TC* (s) *In vivo* (t) BL1 (u) BL2 (v) BL3 (w) Proposed (x) Histology

Conjeti, S., Katouzian, A., Roy, A.G., Peter, L., Sheet, D., Carlier, S., Laine, A. and Navab, N., 2016. Supervised domain adaptation of decision forests: Transfer of models trained in vitro for in vivo intravascular ultrasound tissue characterization. *Medical image analysis*, *32*, pp.1-17.

Take Home Messages

D. Sheet, et. al., "Joint learning of ultrasonic backscattering statistical physics and signal confidence primal for characterizing atherosclerotic plaques using intravascular ultrasound," *Med. Image Anal*,18(1), 2014

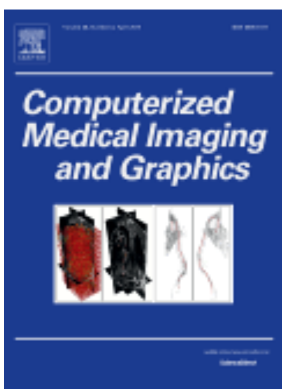

D. Sheet, et., al., "Hunting for necrosis in the shadows of intravascular ultrasound," *CMIG*, 38(2), 2014